

Probing sub-10 nm nanoparticle chemical composition from reactions of methanesulfonic acid with multifunctional amines using thermal desorption chemical ionization mass spectrometry (TDCIMS)

Véronique Perraud, P. S. Bauer, C. E. Miller, P. M. Morris, K. Roundtree, J. N. Smith and Barbara J. Finlayson-Pitts
Department of Chemistry, U. C. Irvine

Introduction

- In air, acid-base chemistry plays an important role in new particle formation (NPF). However, there are still gaps in understanding which species govern this process due to lack of instrumentation to measure chemical composition in the aerosol nanocluster (AN) size range (1-10 nm).¹⁻³

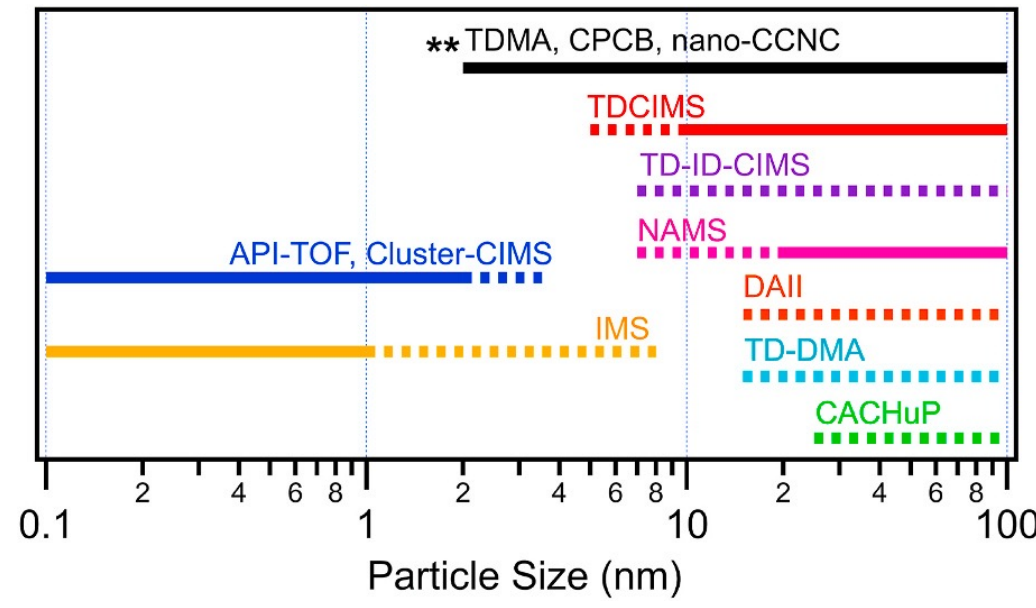
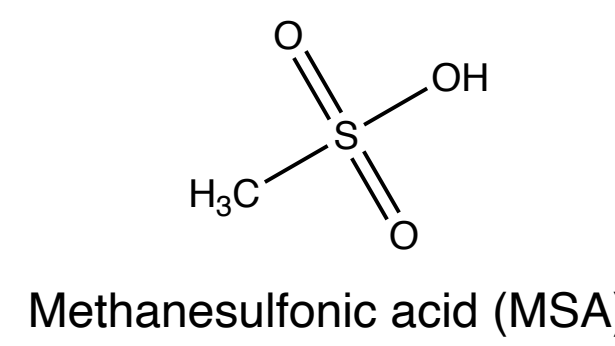
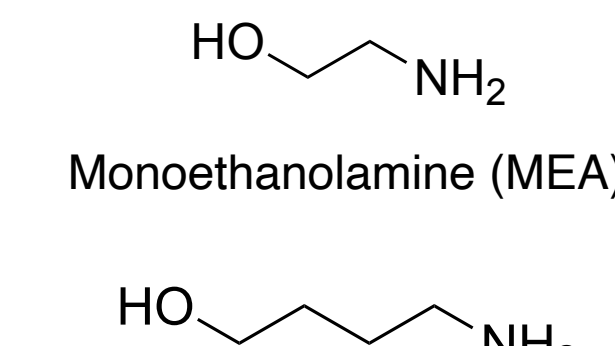


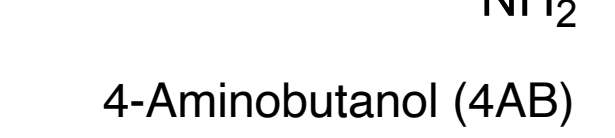
Fig. 1 – Overview¹ of instruments that can measure size-resolved composition in the aerosol nanocluster size range. Solid lines represent ambient measurements and dotted lines are for lab studies. Instruments marked with asterisks (**) measure AN composition indirectly.



- While new particle formation (NPF) is often associated with H_2SO_4 ,^{4,5} there is evidence from field observations that methanesulfonic acid (MSA) can also play a role.⁶ MSA concentrations can be 10-100% that of H_2SO_4 in air,⁷⁻⁹ and the relative MSA contribution to NPF may increase in the future as anthropogenic SO_2 declines worldwide.^{10,11}



- We previously showed that MSA binary reactions with NH_3 or alkylamines can be a significant source of new particles.¹²⁻¹⁷ Reactions with methylamine (MA) in particular are extremely efficient at forming nanoparticles that are neutral above 10 nm, whereas smaller particles are more acidic.¹⁸
- We have extended these studies to multifunctional amines, including two alkanolamines (MEA and 4AB) that are used in carbon capture and storage technology, and are expected to be released into the air.¹⁹



Goal

⇒ Characterize the chemical composition of sub-10 nm nanoparticles and clusters from reactions of MSA with two alkanolamines.

Methodology

Flow Tube Experiments

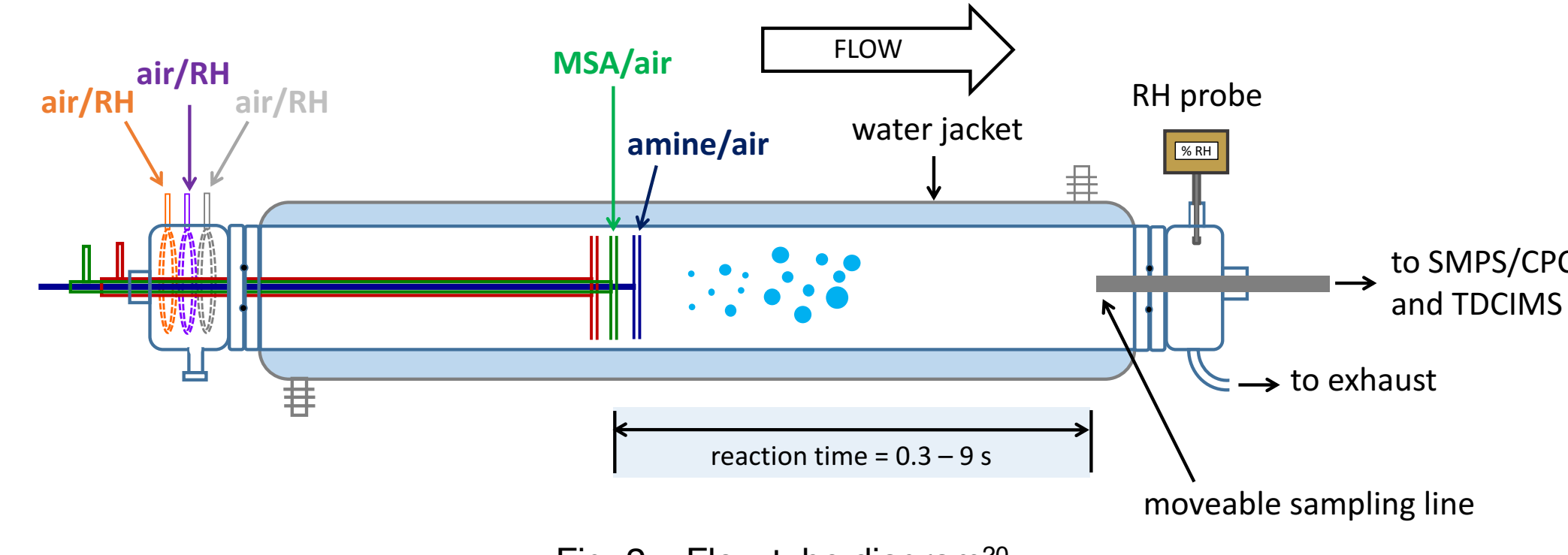


Fig. 2 – Flow tube diagram²⁰

- Experiments were performed at relative humidities ranging from 0% to ~60%.
- Size distributions were acquired at various reaction times using a nano scanning mobility particle sizer (TSI, sheath flow 15 L min⁻¹; aerosol flow 1.5 L min⁻¹).
- Acid:base ratios were measured using thermal desorption chemical ionization mass spectrometry (TDCIMS).^{18,21}

Reactants

- Gas phase MEA/4AB were generated using a diffusion vial method. Their concentrations were measured using ion chromatography²² and UPLC-ESI-MS/MS.
- Gas phase MSA was generated by flowing air over the pure liquid standard maintained in a glass trap. Its concentration was determined by filter collection followed by UPLC-ESI-MS/MS.

Methodology

TDCIMS Measurements

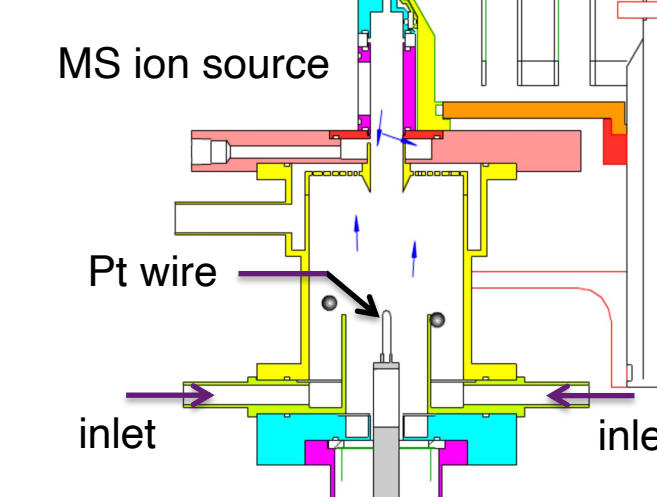


Fig. 3 – schematic of the TDCIMS inlet

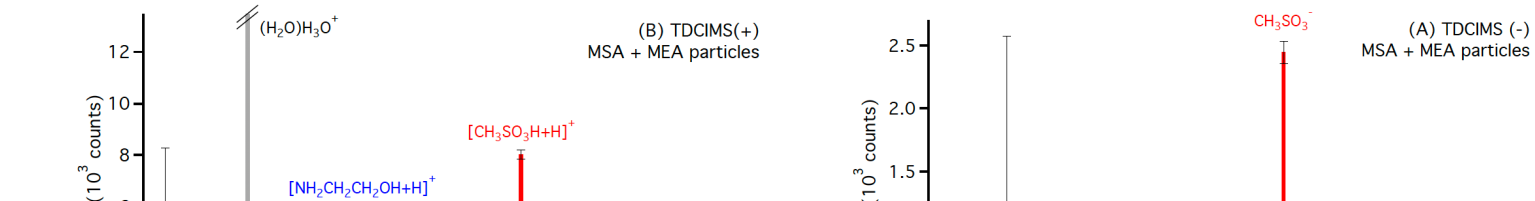


Fig. 4 – MSA-MEA nanoparticles TDCIMS mass spectra

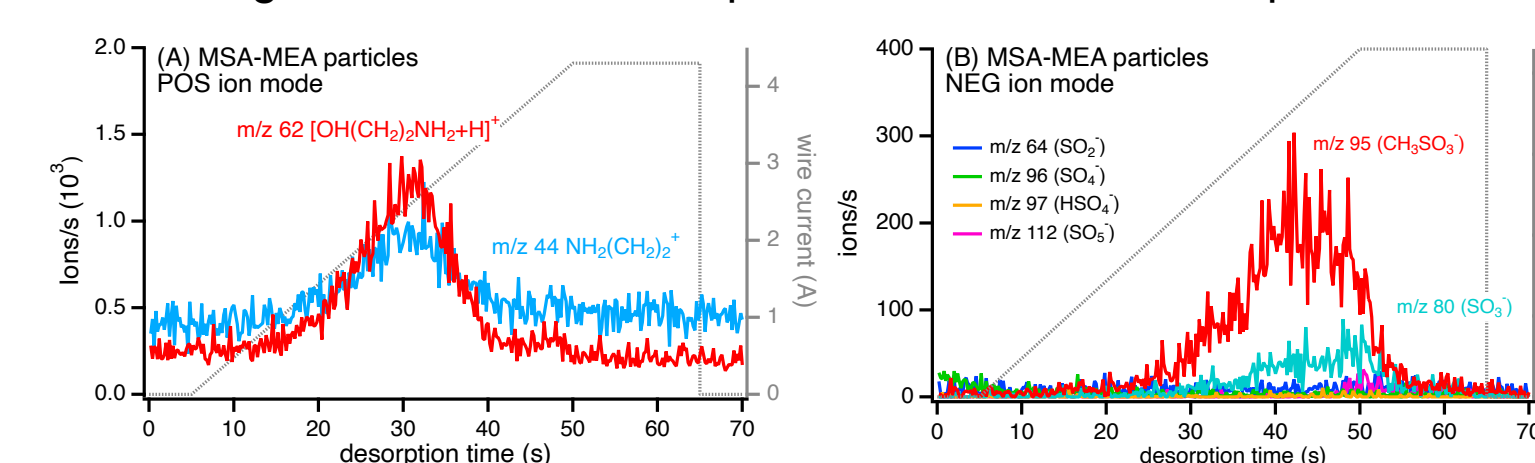


Fig. 5 – Thermodesorption profiles from the analysis of MSA-MEA nanoparticles

- Particles are first charged using a unipolar charger, then size-selected using either a radial DMA or a Half-Mini DMA (SEADM)²⁴ before entering the inlet of the TDCIMS featuring a high-resolution time-of-flight (H-TOF, Tofwerk).
- The TDCIMS measures the size-resolved chemical composition of nanoparticles formed from MSA+MEA and MSA+4AB systems down to ~4 nm.²³

APiTOF-MS Measurements

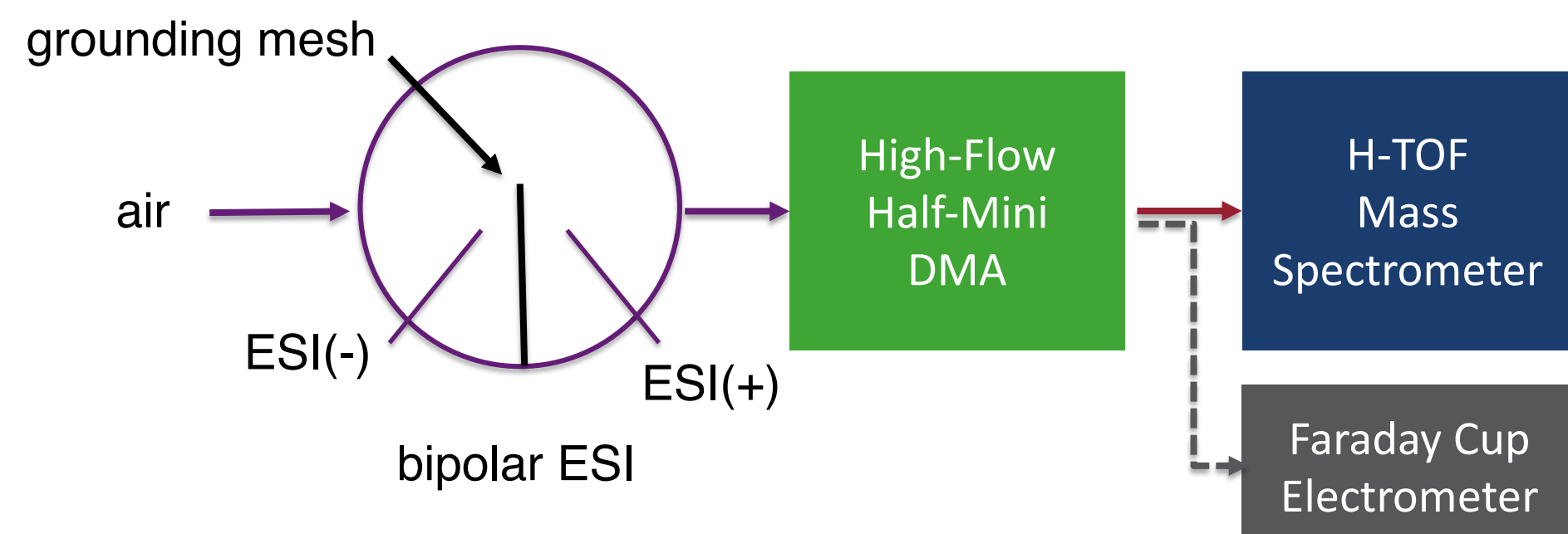


Fig. 6 – Schematic of the bipolar ESI system coupled to the Half-Mini DMA and H-TOF-MS

- To measure the composition of charged clusters < 4 nm, a bipolar ESI system was used in combination with a Half-Mini DMA and the H-TOF-MS.
- Equimolar salt solutions of MSA and 4AB, or MSA and MEA (1.5 $\mu\text{mol mL}^{-1}$) were prepared and sprayed in both ESI(-) and ESI(+). The bipolar spray allows the formation of only singly charged clusters.
- The Half-Mini DMA was operated in both (+) and (-) mode to select negatively and positively charged clusters, respectively, with a sheath flow of ~205 LPM and an aerosol flow of ~8 LPM.
- For analysis, the TDCIMS inlet was removed and the clusters were directly introduced into the inlet aperture of the mass spectrometer.

Results

Flow tube studies

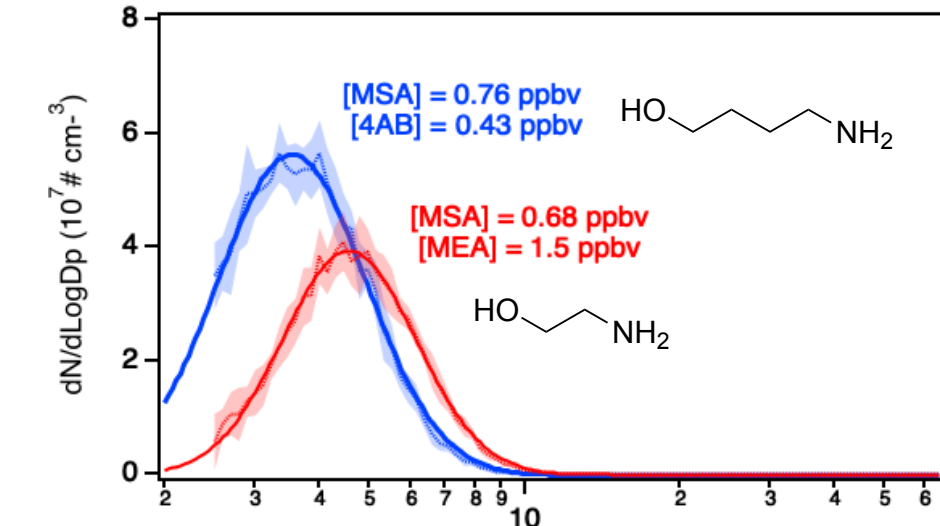
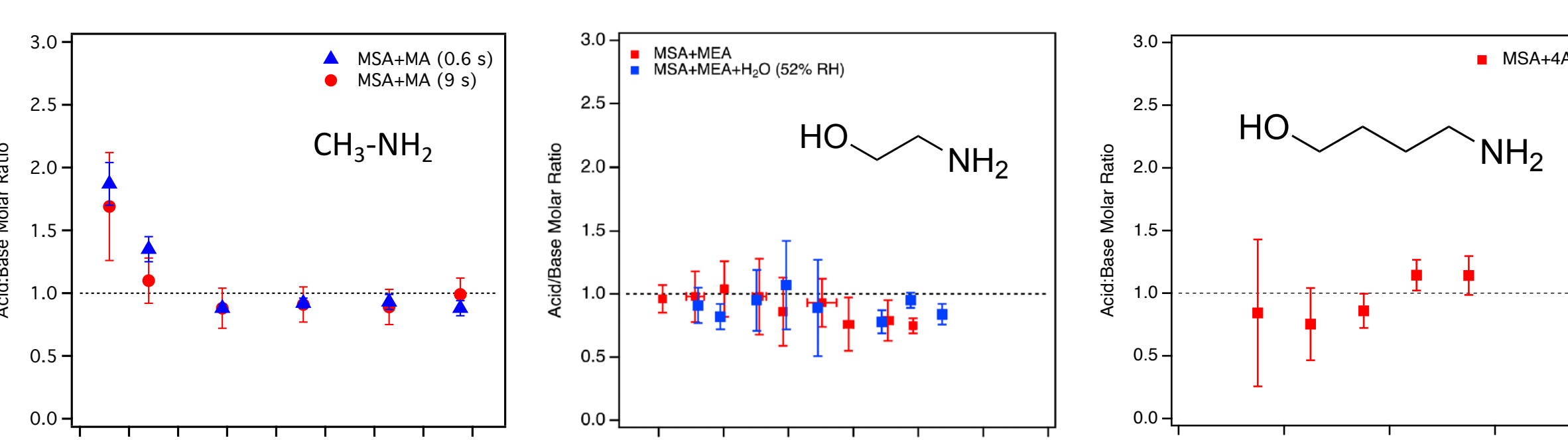


Fig. 7 – Size distributions of MSA-MEA and MSA+4AB particles exiting the flow tube at ~4 s reaction time

⇒ Alkanolamines are extremely efficient at nucleating nanoparticles with MSA, consistent with their high gas phase basicity and $-\text{OH}$ group that increases H-bonding capabilities in the clusters.

⇒ Water has very little influence on these systems.

⇒ More results from MSA+MEA flow tube studies can be found here:²³



⇒ In contrast to MSA+MA,¹⁸ both alkanolamines show an acid:base ratio close to unity with no size-dependence.

Results

Nanocluster studies

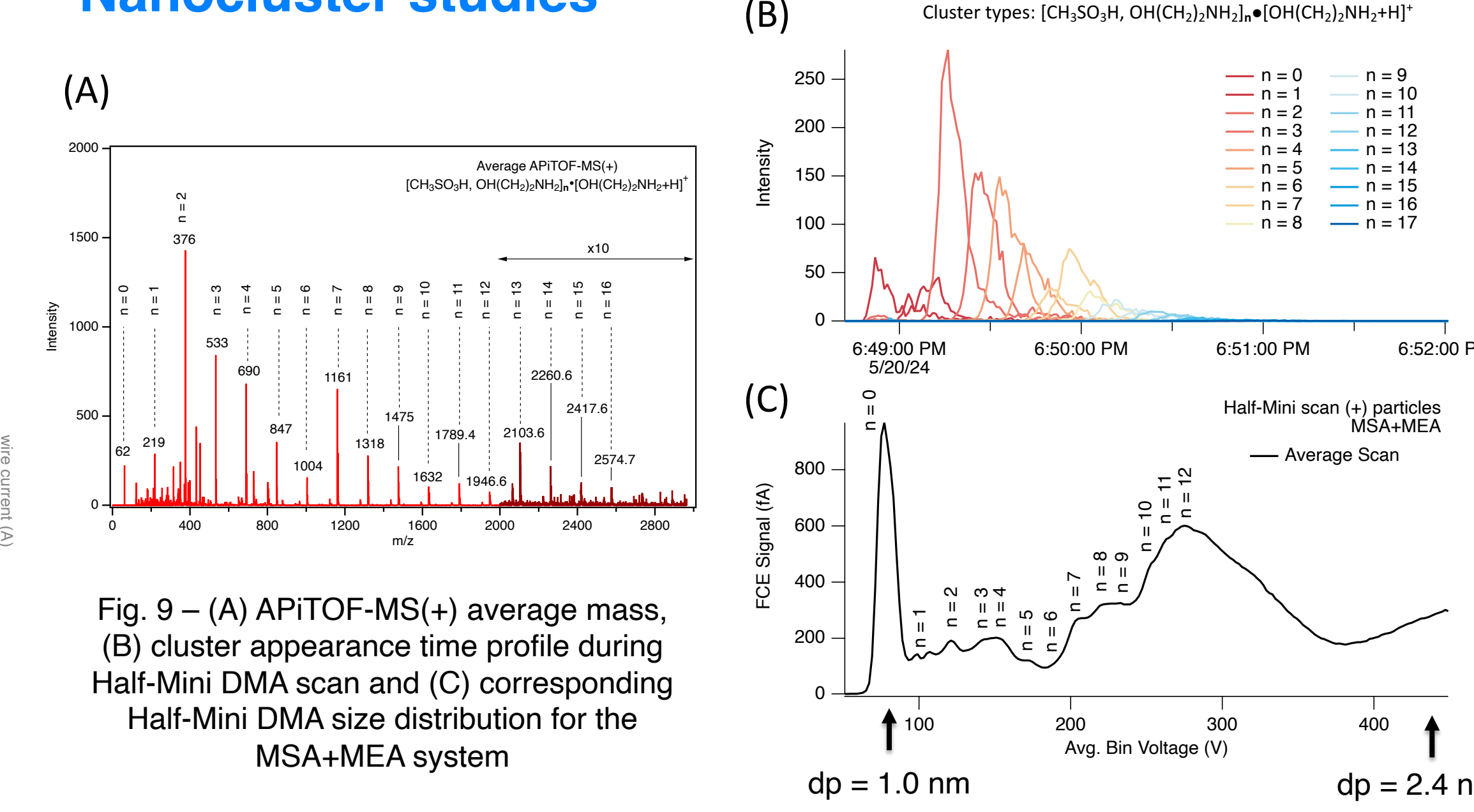


Fig. 9 – (A) API-TOF-MS(+) average mass, (B) cluster appearance time profile during Half-Mini DMA scan and (C) corresponding Half-Mini DMA size distribution for the MSA+MEA system

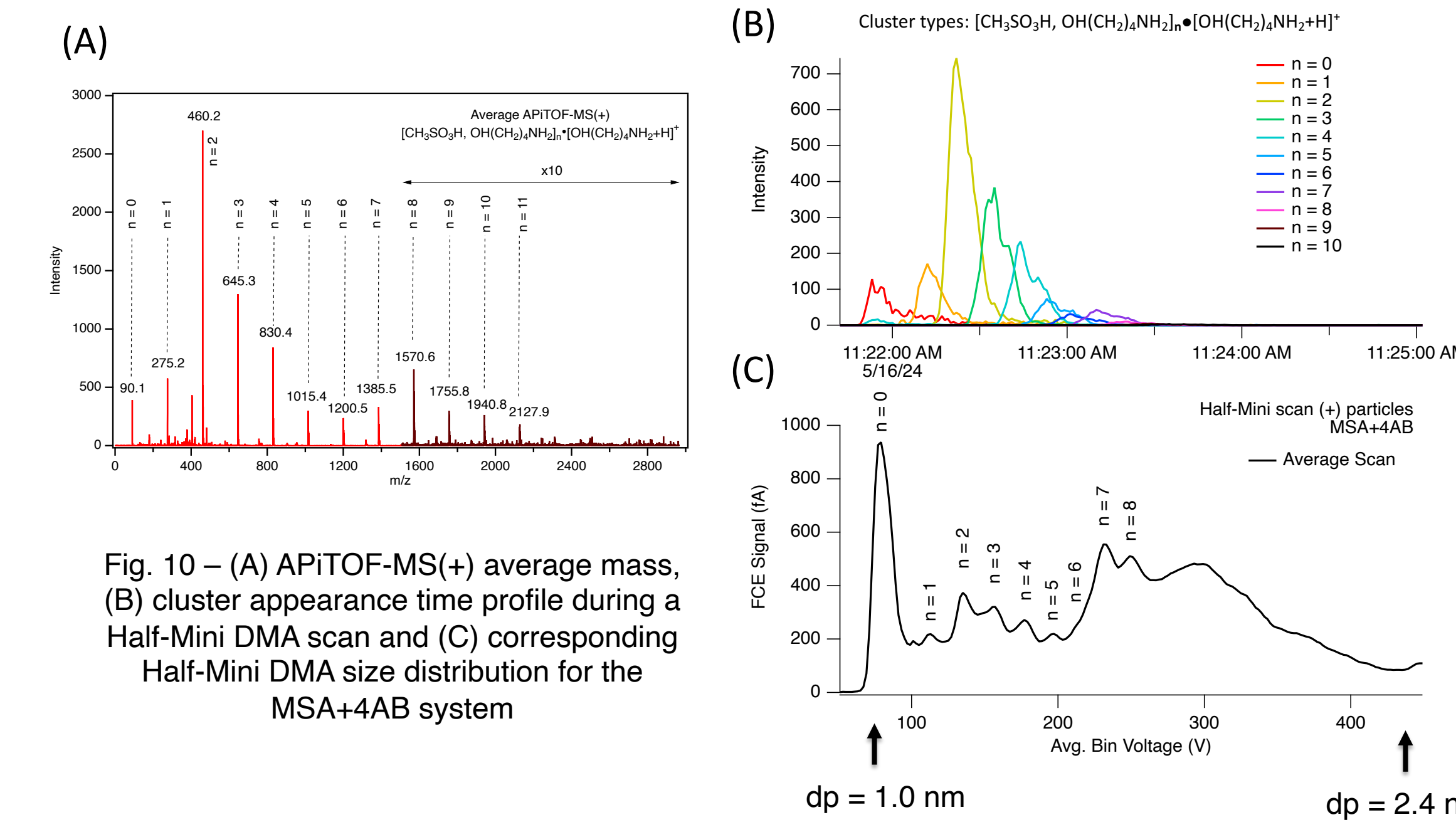


Fig. 10 – (A) API-TOF-MS(+) average mass, (B) cluster appearance time profile during a Half-Mini DMA scan and (C) corresponding Half-Mini DMA size distribution for the MSA+4AB system

⇒ Results from the API-TOF-MS confirm the presence of 1:1 positively charged acid:base clusters for both the MSA+MEA and MSA+4AB systems at the very low size range (< 2.4 nm), consistent with the TDCIMS measurements of particles > 4 nm.

Conclusions

- Flow tube studies show that alkanolamines nucleate particles extremely fast with MSA.
- Both MSA+MEA and MSA+4AB systems form particles with a constant acid:base ratio across all diameters.
- Analysis of sub-2 nm aerosol clusters show similarly a prevalence for the 1:1 positively charged acid:base clusters consistent with the flow tube studies.
- Ongoing work is underway to expand these studies to more multifunctional amines, including a C4 diamine (putrescine) and corresponding simple alkylamine (butylamine).

Acknowledgements

This work is supported by NSF (#1928252 and CHE-2004066) and ARO (#W911NF2010064)

The authors declare no competing financial interest.

References

- Smith et al. (2021) *J. Aerosol Science*, 153, Art No 105733; 2. Lee et al., (2019) *JGR Atmospheres*, 124, 7098-7146; 3. Kerminen et al. (2018) *Environ. Res. Lett.*, 13, Art No 103003; 4. Sipila et al. (2010) *Science*, 327, 1243-1246; 5. Weber et al. (1999) *Geophys. Res. Lett.*, 26, 307-310; 6. Lawler et al. (2018) *Geophys. Res. Lett.* 45 (4) 2038-2046; 7. Berresheim et al. (2002) *J. Geophys. Res.*, 107, doi:10.1029/2000JD000229; 8. Eisele and Tanner (1993) *J. Geophys. Res.*, 98, 9001-9010; 9. Davis et al. (1998) *J. Geophys. Res.*, 103, 1657-1678; 10. Perraud et al. (2015) *PNAS*, 112, 13514-13519; 11. Murphy et al. (2017) *Faraday Discuss.*, 200, 379-395; 12. Dawson et al. (2012) *PNAS*, 109, 18719-18724; 13. Chen et al. (2015) *Phys. Chem. Chem. Phys.*, 17, 13699-13709; 14. Chen et al. (2016) *J. Phys. Chem. B*, 120, 1526-1536; 15. Chen et al. (2017) *Environ. Sci. Technol.*, 51, 243-252; 16. Arquero et al. (2017) *EST*, 51, 2124-2130; 17. Arquero et al. (2017) *PCCP*, 19, 28286-28301; 18. Perraud, Li et al. (2020) *ACS Earth & Space Chemistry*, 4, 1182-1194; 19. Zhu et al. (2013) *Environ. Sci. Technol.* 47, 14306-14314; 20. Ezell et al. (2014) *Aerosol Sci. Technol.* 48 (5), 329-338; 21. Smith et al. (2004) *Aerosol Sci. Technol.*, 38, 100-110; 22. Dawson et al. (2014) *AMT*, 7, 2733-2744; 23. Perraud et al. (2024) *Phys. Chem. Chem. Phys.* 26 (11) 9005-9020; 24. de la Mora and Kozlowski (2013) *J. Aerosol Sci.* 57, 45-53.